

IAC-24-A.1.2.3

Space-Based Solar Power for Operational Robustness in Lunar EVAs and Exploration Architectures

Madelyn Hoying^{a*}, Anna Tretiakova^b, Vanessa Z. Chen^c, Clara Ma^d, Palak B. Patel^e, Lanie McKinney^f

^a MIT-Harvard Medical School Health Sciences and Technology, MIT Department of Aeronautics and Astronautics, Wellman Center for Photomedicine, Massachusetts General Hospital,

^b Boston University Mechanical Engineering,

^c University of Waterloo Biomedical Engineering,

^d MIT Department of Aeronautics and Astronautics, Technology and Policy Planning,

^e MIT Department of Mechanical Engineering,

^f MIT Department of Aeronautics and Astronautics,

* Corresponding author

Abstract

Human exploration of the lunar surface has large power requirements for both the lunar base and for rover exploration. NASA's recent contract awards indicate a reliance on fission surface power. While nuclear options provide reliable power to lunar base locations, they have a limited reach that restricts exploration capacity. The Space Exploration Vehicle's 125-mile range only allows coverage of 0.34% of the lunar surface. A constellation of space-based solar power (SBSP) satellites paired with pressurized rovers allows 24-hour, full-surface coverage on excursions from the lunar base. Instead of narrowing exploration and science capabilities to the area around the base, preliminary analysis indicates the ability to extend a surface campaign's capabilities to full-surface coverage with 30 satellites in a 3 plane Walker-Delta Constellation with 54.7° inclination. This also provides dissimilar redundancy in the lunar surface power supply to add robustness to the overall mission architecture by providing an alternative method of powering the life support and critical power needs of the habitat in an emergency. A case study of constellation design, cost, lifetime, and power provided is conducted. In this study, we evaluate the impact of the additional exploration capacity on the MARTEMIS mission concept, which was named Best in Theme in the 2024 NASA RASC-AL design competition. MARTEMIS includes a campaign of 13 manned surface missions intended to evaluate architectural decisions and critical technologies for future Mars missions. Throughout the campaign, 148 astronauts will visit the lunar surface and conduct 332 EVAs. This campaign has the potential to significantly advance NASA's lunar science objectives while demonstrating Moon to Mars operations and technologies. A 125-mile EVA radius from a South Pole base reaches up to 8 of the 48 lunar geologic units; lunar science objectives target widespread sampling across all geologic units. The proposed SBSP constellation spreads the 332 EVAs across the areas of scientific interest instead of constraining exploration to the landing site. It has the additional benefit of increased operational safety and robustness in emergency scenarios. Addition of a SBSP constellation for rovers provides operational flexibility, safety, and robustness to enable multiple lunar exploration architectures beyond that enabled by surface power infrastructures.

1. Introduction

Maintaining human habitation and exploration on a planetary surface requires large power inputs, with projected power demand for a 4-person crew on the lunar surface peaking at 100 kWe [1]. With NASA's Moon to Mars Objectives, nuclear fission power has been prioritized as the main energy source to meet this demand [2, 3]. NASA's Artemis program includes development of a 40 kWe reactor[4], and larger fission power reactors are in development for Earth use[5, 6]. Fission power meets several key requirements for human exploration of Mars, including:

- reliable, weather-independent power production

- terrain-independent power production
- overcoming the reduced productivity of solar power at Mars distances from the Sun.

The comparison between fission power and surface solar power has been well documented [7, 8], particularly for architectures on Mars or using the Moon as a testbed to develop technology for Mars. However, space-based solar power (SBSP) provides an attractive alternative that has only begun to be explored[9], particularly as an option in lunar architectures.

Here, we explore the inclusion of SBSP alongside surface fission power to provide dissimilar redundancy and

operational robustness in large-scale human lunar exploration architectures. The current architectural decision to rely on fission power presents a single point of failure; a catastrophic event in the fission power production system could result in a critical failure where the habitats, life support systems, and critical crew functionalities are left with no power.

Ensuring both system-level reliability and operational robustness in power systems relies on introducing dissimilar redundancy. This can be achieved by using a combination of fission surface power and SBSP. Fission surface power meets the needs of powering a lunar base, in that the power supply system and infrastructure can be well established at a permanent location near the base without constraining site selection. SBSP can enhance safety by ensuring additional power generation capacity to accommodate overflow or unexpected surges in the lunar base's power demand. Together these systems ensure architecture-level operational robustness that includes an ability to maintain operational performance after a single failure[10].

SBSP also allows prioritization of widespread lunar exploration that is otherwise constrained by the localized infrastructure associated with fission or other surface power alternatives. In addition to exploring the SBSP tradespace for operational robustness of the lunar habitat, we present a constellation design that targets full lunar surface coverage to enhance the exploration and science capabilities towards a future permanent lunar presence, with the ability to accommodate evolving EVA requirements.

2. MARTEMIS Overview

The multi-mission MARTEMIS campaign, presented in more detail in [11], provides the case study for the SBSP constellation and analysis conducted here. The MARTEMIS concept won Best in Theme at the 2024 NASA Revolutionary Aero-Space Concepts Academic Linkage (RASC-AL) competition. A recommended campaign architecture of 13 missions with a total of 154 crew (labeled 13-154) was selected through a trade study of 23 alternative architectures with varying crew size, surface time, transit time, and margin parameters. An overview of the surface campaign can be seen in Figure 1. This architecture balances the estimated lifecycle cost with metrics for the elimination of knowledge gaps, the degree of international participation, crew time available for science, and commercial alignment. Standard Taguchi Orthogonal Arrays [12] were used to optimize the 13-154 campaign architecture for efficient knowledge gap closure within the available surface time. This method indicates that of the 13 missions, 10 are required to inform architectural decisions for a Mars mission (termed the "MARTEMIS prime" missions). The remaining 3 are missions of opportunity

for additional testing beyond the crew size, surface and transit time, and margin variables, at minimal additional lifecycle cost.

MARTEMIS consists of a full mission architecture, including designs for surface habitats, rovers, and supporting infrastructure; it also sets forth a framework for the surface science experiments to be conducted in accordance with the NASA Moon to Mars objectives and the stated goals of international partners [2]. Notably, the selected power production methods include a combination of surface fission power and SBSP to provide operational robustness through dissimilar redundancy, as well as enhance the exploration capabilities of the campaign. Here, we explore the addition of SBSP in detail, with an emphasis on meeting NASA's lunar exploration targets through the extended EVA range.

2.1 EVA Allocations

MARTEMIS distinguishes two categories of EVAs:

1. Short EVAs last less than 6 hours and are located no more than 10 km away from the base, and can be reached on foot or via rover.
2. Long EVAs can last up to 30 days and explore sites up to 1000 km away from the base (as calculated in Section 2.2). During these EVAs, the habitable rover provides the astronauts a pressurized habitat in which to sleep, to rest, and to eat without suits.

EVA planning is calculated using the following principles, driven by crew safety and science return requirements for the MARTEMIS campaign:

1. Each long EVA lasts a maximum of one month and requires 2 rovers with 2 crew members each.
2. The crew participating in long EVAs rotate each month, allowing for recovery time.
3. Each short EVA lasts a maximum of 1 work day and can occur once per week.
4. Multiple EVAs can occur simultaneously.
5. 2 or more crew members remain at the base habitat.
6. Because of the greater science return of long EVAs, these are calculated first. The remaining time is assigned to short EVAs.

These principles give the following equations to allocate EVA time:

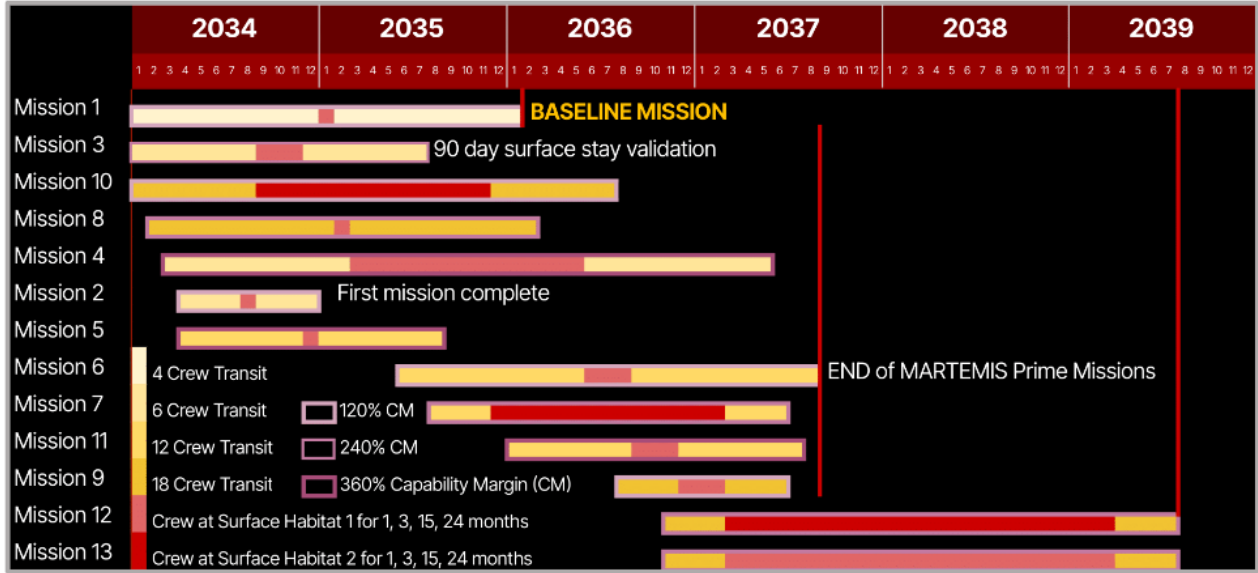


Fig. 1. MARTEMIS 13-154 campaign Concept of Operations, reproduced with permission of the authors from [11]. The order of missions is designed to minimize total campaign time while optimizing habitat occupancy. The MARTEMIS prime missions (1-10) are prioritized in the schedule to adhere to NASA’s target dates for a manned Mars mission.

$$\#_{LongEVA_s} = \begin{cases} M \times \left(\lfloor \frac{C}{4} \rfloor - 1 \right), & C - 4 = 0 \\ M \times \lfloor \frac{C}{4} \rfloor, & C - 4 \neq 0 \end{cases} \quad [1]$$

$$\#_{ShortEVA_s} = \begin{cases} \left\lceil \frac{M}{2} \times \left(\lfloor \frac{C}{4} \rfloor - 1 \right) \right\rceil, & C - 4 = 0 \\ \left\lceil \frac{M}{2} \times \lfloor \frac{C}{4} \rfloor \right\rceil, & C - 4 \neq 0 \end{cases} \quad [2]$$

where M denotes the surface stay duration in months and C is the crew size. Note that the symbol $\lfloor x \rfloor$ denotes rounding down to the nearest integer, while $\lceil x \rceil$ indicates rounding up to the nearest integer.

For a 12 person crew, for example, four people can conduct a long EVA at once, with remaining crew eligible for the next EVA. The length of each short and long EVA within the upper bounds described here depends on the complexity of scientific tasks to be performed, suiting time, and depressurization time. Calculated EVA numbers for the representative 13_154 campaign are shown in Table 1, tallying 332 long and 124 short EVAs over 109 months of surface mission duration.

2.2 Science Targets on EVA

EVA allocations are dependent on the crew size and mission duration per Eqn. 1 and 2. The number of EVAs set to be conducted in a mission therefore remains constant with introduction of SBSP. However, the exploration plan can change drastically within the EVAs by introducing SBSP due to changes in rover range. Assuming a set 30-day rover habitability window, the expected EVA range can be calculated using both SBSP and base surface power.

For a long EVA, the sites visited are divided into high and low workload sites. At low workload sites, samples can quickly be gathered, or a site can rapidly be evaluated. High workload sites, on the other hand, require intensive physical preparation to collect samples, such as those inside of craters. Low workload sites may require EVAs of up to 6 hours, while high workload sites require up to 12 hours. In 30 days with 8 hours of sleep per day, the astronauts have 480 working hours. After subtracting EVA time based on Equations 2 and 1, the remaining time allows for a driving speed averaging 5 km/h towards the final destination. Although the actual driving speed of the rover may exceed 14 km/h [13], time is allocated for stopping, pathfinding, navigating rough terrain, and hazard avoidance.

With SBSP, this gives a maximum exploration radius of 1000 km. For any destination at a radius of 1000 km

Mission #	# of Crew	Surface Stay (Months)	# of Short EVAs	# of Long EVAs
1	4 (2 on surface)	1	0	1
2	6	3	0	3
3	18	15	0	60
4	18	1	0	4
5	6	15	0	15
6	6	1	0	1
7	12	1	2	2
8	12	3	86	6
9	12	15	30	30
10	12	3	6	6
11	18	3	0	12
12	18	24	0	96
13	18	24	0	96
Total:	160	109	124	332

Table 1. The total number of EVAs to be completed for each mission in the 13_154 reference architecture, calculated using Eqn. 1 and 2 [11].

from the MARTEMIS South Pole base habitat, the crew will encounter an average of six different of geologic regions (low workload sites) and three craters (high workload sites). With standard surface power at the base location, though, rovers are predicted to reach 25 km before requiring a return to base for charging [14], with a maximum range predicted at 125 km [15]; this significantly limits the exploration capacity of the mission. With SBSP, the EVA range increase comes with increased science capacity; the 125 km range provides access to 8 of 48 lunar geologic units, while 1000 km reaches 26 [16]. For a large architecture like MARTEMIS with hundreds of EVA opportunities, this drives the need for SBSP as a science- and exploration-enabling technology.

3. Constellation Design

3.1 Key SBSP Requirements

MARTEMIS targets an energy architecture with system redundancy, autonomous operation, and long service intervals [11]. SBSP is a component of this energy architecture; it provides critical system redundancy, complementary to the surface power generation infrastructure. It also enhances the ability to meet surface exploration objectives designated by MARTEMIS. The SBSP architecture therefore must provide full-surface lunar coverage with the ability to provide backup power to the habitats and charge rovers quickly.

3.2 Orbital Geometry Selection

The minimum number of satellites needed for full coverage per orbital plane assuming a circular orbit, or S_{min} , is given by [17]:

$$S_{min} = \left\lceil \frac{\pi}{\cos^{-1}\left(\frac{R_l}{R_{sat}}\right)} \right\rceil \quad [3]$$

where R_l is the lunar radius and R_{sat} is the radius of the satellite's orbit with respect to the center of the moon, or $R_{sat} = R_l + \text{altitude}$. We want to look at scenarios using discrete numbers of satellites to evaluate the SBSP tradespace with regards to system cost and requirements met; rewriting this equation as an inequality allows us to solve for R_{sat} with given S_{min} values. The inequality

$$S_{min} - 1 < \frac{\pi}{\cos^{-1}\left(\frac{R_l}{R_{sat}}\right)} \leq S_{min} \quad [4]$$

when solved for R_{sat} gives

$$R_l \sec\left(\frac{\pi}{S_{min} - 1}\right) < R_{sat} \leq R_l \sec\left(\frac{\pi}{S_{min}}\right). \quad [5]$$

Calculations for R_{sat} with S_{min} ranging from 1-30 were completed, constraining the allowable semimajor axis a within upper and lower limits to enable full surface coverage. Results are shown in Table 2.

Lunar orbit selection must also account for lunar mass concentrations (mascons); these are gravitational anomalies that produce orbital perturbations particularly at low lunar orbits [18]. There are several stable "frozen" orbits which do not require orbital corrections due to mascons [19]. Results in Table 2 were compared to these frozen orbits. We select a frozen circular orbit with inclination of 54°, true anomaly ω of 90°, and a of 1861 km; this fits within the calculated limits of a for 9 or greater satellites

Satellites per Plane	a , Upper Limit (km)	a , Lower Limit (km)
1	-3228.431	-1740.002
2	2066.751	2185032.822
3	1741.896	3476.804
4	1781.005	2459.752
5	1867.750	2150.261
6	1958.292	2008.871
7	2042.788	1931.043
8	2119.166	1883.207
9	2187.549	1851.550
10	2248.684	1829.450
11	2303.442	1813.381
12	2352.651	1801.317
13	2397.041	1792.020
14	2437.244	1784.701
15	2473.799	1778.832

Table 2. Calculated orbital parameters for a given S_{min} . Constellations using an S_{min} of 6 or less result in an a upper limit that is lower than the lower limit; as such, the lowest allowed S_{min} is 7.

Satellite Constellation Illustrated in Isentropic View

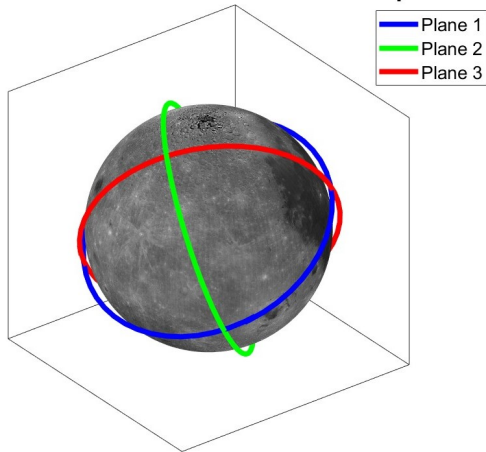


Fig. 2. Isentropic view of the selected constellation.

per orbital plane.

We further propose use of 3 orbital planes in a Walker-Delta configuration. The 3-plane Walker-Delta constellation with a 54.7° inclination is particularly effective at delivering comprehensive coverage around a celestial body by optimizing satellite visibility across all latitudes, including polar regions.

To prioritize system-level robustness, we select a constellation design with 10 satellites per plane such that a one-out analysis still ensures full operational capability of the constellation. In other words, 10 satellites per plane in

the selected orbit only requires 9 for full surface coverage. If one satellite fails in any or all of the orbital planes, the architecture’s operational capacity does not change. This totals 30 satellites and strategically distributes these satellites across multiple orbital planes, ensuring continuous communication and observation capabilities.

The constellation and full orbit of all 30 satellites were simulated using MATLAB R2024a. Figure 2 illustrates the constellation in isentropic view. In order to demonstrate the constellation’s full coverage, a few locations on the moon were selected: the Apollo landing sites, and the four outermost proposed Artemis landing sites. Figure 3 shows the orbital tracks and charging coverage circles with these representative points of interest on the lunar surface.

3.3 Constellation Lifecycle

MARTEMIS concept of operations includes 9 years of lunar power system operation, with optional extensions following infrastructure transition to industry on conclusion of the campaign. Constellation deployment begins in 2030 and crew operations begin in 2034, with all missions complete in 2039.

The decision to design this constellation for full lunar surface coverage was made in anticipation of evolving future requirements set by industry or NASA missions of opportunity, to provide power as we further investigate new areas of the lunar surface for commercial or scientific purposes. As such, this constellation is intended to persevere well beyond the 9-year MARTEMIS timeline. End-of-life operations following industry use are an area for future analysis.

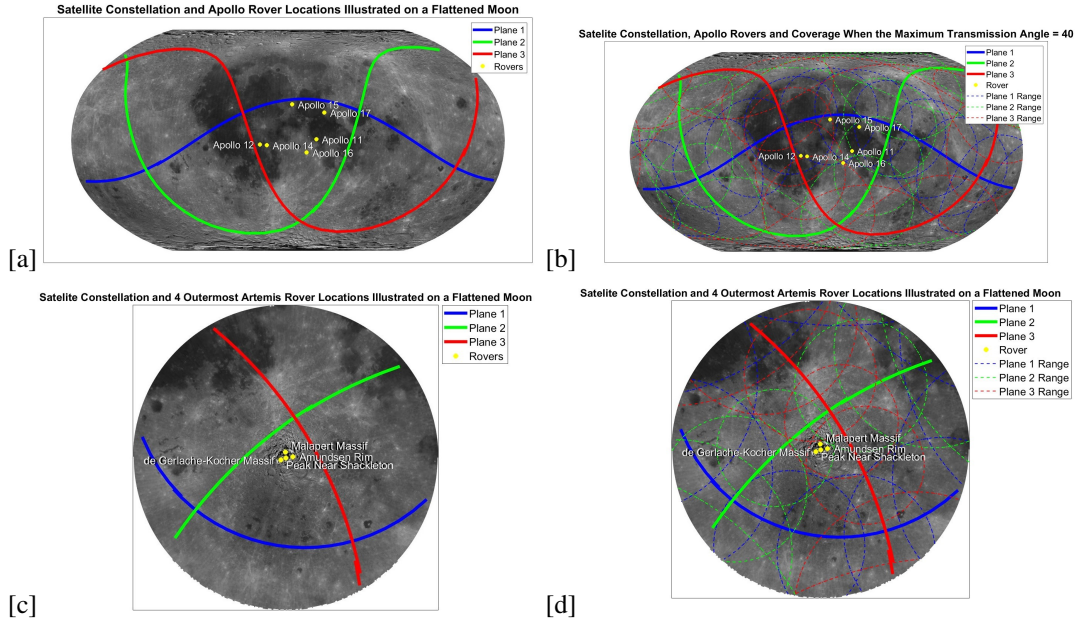


Fig. 3. Apollo (a, b) and Artemis (c, d) landing site coverage with the proposed constellation. [b] and [d] illustrate the satellite coverage when the transmission angle is 40 degrees.

4. Satellite Bus Components

Each satellite in the constellation will be equipped with a laser for laser power transmission (LPT), a battery to power the satellite as well as store the power that is being transmitted, a thermal control system, focusing system, and solar panels. The main role of this satellite is to utilize LPT to charge rovers on the surface of the moon using solar power.

4.1 Laser Power Transmission (LPT)

LPT works by converting electrical energy into electromagnetic energy for transmission, and then back to electrical energy at the receiver [20]. LPT is selected over microwave power transmission due to the ability of the laser to make a very concentrated beam of energy that dissipates less, making it more effective over long distances [21]. While initially more costly, LPT is also more compact with lower mass.

The analysis that follows uses a ytterbium-doped fiber laser with wavelength = 1064 nm, peak power = 30 kW, electrical efficiency = 50%, and waist radius = 250 mm, with a TRL of 3 [21]. This has strong absorption (at 976 nm) and emission (1030–1100 nm), making it an efficient medium for converting pump light from laser diodes into laser light. Fiber lasers are also very scalable; while this design utilizes one fiber laser, there is opportunity to scale up for higher orbits or otherwise increased transmission requirements.

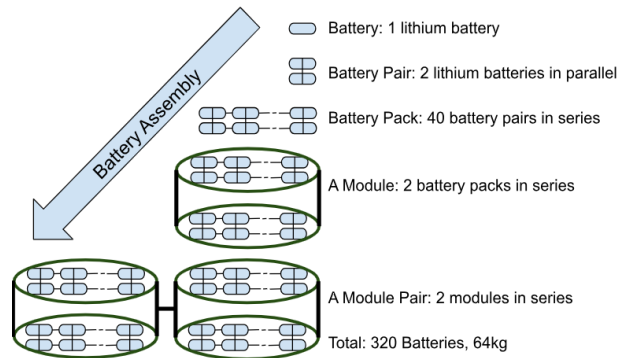


Fig. 4. Battery system structure as described in [9].

4.2 On-Board Battery

The battery system chosen follows [9] for lunar SBSP. The battery system is made up of 320 small lithium ion battery units weighing a total of 64 kg, as shown in Figure 4. In standard operation, the batteries charge via solar panels while exposed to the sun and discharge when in the cone of a receiver on the surface; more advanced charge cycling methods can be applied to extend battery life of the rover, as discussed in Section 5.1. Additionally, the satellite battery lifespan is extended by designating the charge state to remain within 10-90%.

The battery system therefore provides a cell capacity of 20 Ah, thermal mass 400 J/K, coolant thermal path re-

sistance 1K/W, ambient thermal path resistance 20 K/W, voltage 4V and initial charge 0.3 amps. The life span is 10 years with an efficiency of 0.65 when energy is transferring from solar panels to batteries and an efficiency of 0.85 when energy is transferring from batteries to the laser. The solar array area must be 26 m^2 to charge the battery for LPT and to power the onboard systems [9].

4.3 Thermal Control System

Lasers, especially high-power and precision lasers, generate significant heat during operation. This can lead to thermal-induced damage, performance degradation, and reduced operational lifespan; proper thermal control system selection is therefore crucial to SBSP design. We select the oscillating heat pipe method, as it is a TRL 6 technology that minimizes thermal gradients and prevents hotspots that could damage components [22].

4.4 Pointing and Targeting System

The selected orbital altitude a means that the laser will not only have to be powerful, but also very accurate. The fine guidance sensor used on the Hubble telescope has the ability to point at a target with an accuracy of 0.01 arcsecond, and has the ability to remain pointing at the target with a drift of 0.007 arcseconds per day. This is selected with a TRL of 9 [23].

5. Rover Charging Capabilities

5.1 Surface Receivers

In the MARTEMIS architecture, an LPT receiver is included on the habitat and on each rover. The habitat receiver remains on nominally for use as a backup or supplemental power supply.

The rover receivers are intended to be turned on when stationary and off while moving, when possible. This is to avoid jumps between charging and not charging states as the rover crosses coverage zones. Once parked at an EVA site, the receiver is turned on and the rover is recharged via normal satellite movement over the receiver cone. Operationally, this works well for EVAs with periodic pauses for sample collections in order to avoid incurring wait times for rover charging. For long EVA drives without charging breaks, a strategic power cycling method is applied to extend the lifespan of the rover batteries. For example, a rover is driven until discharged to 20%, and then a receiver is turned on to charge while driving until reaching full charge; the receiver is then turned off until stopping or reaching 20% charge again.

Unlike the wide range of light that can be absorbed by standard solar panels, LPT receivers are designed to only absorb the light from the laser used in transmission. The receiver is a photovoltaic cell and works by matching

the band gap of the material to the energy of the photon it is trying to absorb. The better the match, the higher the conversion efficiency. Commercial advances in this field have achieved a conversion efficiency of $68.9 \pm 2.8\%$ under 858 nm monochromatic light with gallium arsenide photovoltaic cells at a TRL 2 [24].

5.2 Wireless Power Transmission (WPT)

Zheng et al. concluded that, for our selected constellation, the average power transmitted to each receiver in a single hour by the entire plane of 10 satellites is 6.45 kW [20]. This means that each satellite that is over a target location supplies the receiver with 0.2 kW every two minutes.

6. Power Output

The constellation design was selected to distribute satellites across multiple orbital planes for global WPT coverage as described in Section 3. The coverage at representative sites of interest was therefore modeled to evaluate whether this constellation meets the coverage requirements. Using MATLAB R2024a Lunar Orbital Propagation tool, the exact times of when each satellite enters and leaves the transmission cone of each chosen location were calculated and used to derive the time required to charge a rover. Four of the outermost proposed Artemis landing sites [25] were selected as sites of interest to demonstrate how this constellation design will power the main habitat area. To further demonstrate exploration capabilities, four Apollo landing sites [26] were modeled as well; of note, the Apollo 16 site demonstrates coverage in the overlap of all three orbital planes. Appendix A shows a breakdown of which satellites in the constellation are over a given location in two-minute intervals, over a representative two-hour time frame. This is used to calculate the power delivered to a receiver over the span of a complete orbit, shown in Appendix B. Figure 5 shows the expected power output per two-hour orbital window at the selected locations.

In the proposed Artemis locations, there will be a stable power supply of 36-40kW with every two-hour orbital cycle; this provides emergency power for critical habitat systems, while fully supporting EVA operations in the habitat area in nominal scenarios. The constellation provides more than 15 kW/h globally, reaching a minimum near the lunar equator. These calculations indicate that it would take no more than 2.5 hours to fully charge the rovers in all of the representative locations, assuming that the rover batteries will have similar properties to standard Earth electric vehicle batteries [27]. This charging period fits well within the EVA structure outline in Section 2.2, indicating that the constellation design meets MARTEMIS requirements.

Apollo Location	Percent of Time Spent Over Top of Location			All Planes	Overlap?	Total Power (kW)
	Plane 1	Plane 2	Plane 3			
Apollo 11	0.150	0.154	0.000	0.304	no	38.8
Apollo 16	0.048	0.144	0.100	0.291	no	31.400
Apollo 12	0.154	0.000	0.207	0.361	no	39.000
Apollo 17	0.206	0.159	0.000	0.365	no	39.400
Artemis Location	Plane 1	Plane 2	Plane 3	All Planes	Overlap?	Total Power (kW)
Malapert Massif	0.000	0.185	0.185	0.370	yes	40.000
Peak of Shackleton	0.000	0.185	0.185	0.370	yes	40.000
Amundsen Rim	0.000	0.167	0.189	0.356	yes	38.400
de Gerlache-Kocher Massif	0.000	0.185	0.189	0.337	yes	36.800

Fig. 5. Summary of the total power delivered to the representative receiver locations and the percentage of time spent in the receiver cone over the location, out of each two-hour orbital cycle.

7. Affordability in Large Mission Architectures

The total lifecycle cost C of the MARTEMIS campaign is calculated as follows [28, 29]:

$$C = (C_{assets} + C_{ops} + C_{launch}) \times 1.4 \quad [6]$$

where 1.4 is a factor added for 10% of mission costs allocated to education and outreach plus a 30% margin.

The cost for all of the mission assets C_{assets} , including surface, orbital, and mobility assets, is defined as:

$$C_{assets} = \sum_{t=1}^T (D_t + U_t C_{f,t}) \quad [7]$$

where T is the number of types of unique technology developments, D_t is the DDT&E cost, U_t is the number of repeat units of an element type t , and $C_{f,t}$ is the unit fabrication cost.

Operational costs, C_{ops} , are defined as:

$$C_{ops} = N_s (Y_{pre} + Y_{surface}) C_o \quad [8]$$

where N_s is the number of operations staff for the architecture, Y_{pre} is the number of operational years of the architecture excluding surface operations, $Y_{surface}$ is the number of surface endurance years, and C_o is the average annual cost per staff member.

Launch costs, C_{launch} , are defined as:

$$C_{launch} = C_L (L_{pre} + L_{crew} + L_{cargo} + L_{other}) \quad [9]$$

where C_L is the average cost per launch, and L_{pre} , L_{crew} , L_{cargo} , and L_{other} is the number of precursor or pre-mission launches, crew launches, cargo launches, and all other launches (including tanker/refueling launches), respectively.

From these calculations, it can be determined that adding a single unique asset, in this case an SBSP satellite, has a minimal impact on overall mission cost of large-scale mission architectures. The MARTEMIS representative 13_154 architecture's lifecycle cost was calculated to be \$91B; with anticipated cost-sharing and international partnerships, the cost to NASA was estimated to be \$25B [11]. A constellation of 30 SBSP satellites adds a system cost of approximately \$720M following the same cost model. This adds 0.79% to the total mission campaign budget.

8. Areas for Future Analysis

In Section 3.2, we provide a preliminary orbital analysis to determine a notional constellation design. More complex orbital analyses have been conducted to optimize for lunar navigation mission requirements [30]; these procedures should be applied to lunar SBSP. For example, multi-orbit constellations can optimize for full surface coverage with fewer satellites than single-orbit constellations [31]. This could reduce the cost of the SBSP system and increase its desirability in smaller mission architectures. Additionally, detailed considerations of other orbital mechanics parameters are needed, including the impact of sun geometry on charge time and the impact of perturbations (such as lunar gravity and solar radiation pressure) on lifecycle.

Technical aspects of SBSP need further development for TRL progression. For example, fiber lasers for LPT provide areas for future optimization; if waveforms are coherent, their intensity scales as n^2 , where n is the number of fiber lasers. If the waveforms are not coherent, which may arise due to satellite size constraints, then the intensity scales as $\sum n$ [32]. Advanced laser configurations such as that given by the tiled-aperture method [32] should be investigated to determine spacing for maximum inten-

Metric	Without SBSP	With SBSP
Emergency Power Supply	Fission Power Only	Additional 20 kW/h
EVA Maximum Range	125 km	1000 km
EVA Lunar Surface Coverage	8 geologic units	26 geologic units
Added Lifecycle Cost	-	0.79%

Table 3. MARTEMIS mission performance with the addition of SBSP.

sity and efficiency. More work is needed to develop the surface receiver technology and demonstrate the use of WPT in exploration.

Adding SBSP infrastructure for lunar exploration could have important implications in future mission architecture selection. Rovers with longer habitability windows (>30 days), or even fully mobile habitats, could become a desirable exploration architecture. The limitation on surface exploration is 1000 km in MARTEMIS, driven entirely by the habitability duration of the rover. With SBSP, we have reliable global power accessibility with built-in similar redundancy, reducing one risk to mobile lunar habitat architectures [33]. Trade studies are needed to evaluate mobile versus fixed base architectures for science output.

9. Conclusions

SBSP provides critical system redundancy and enables far-reaching exploration in lunar architectures. For just a 0.79% increase in MARTEMIS campaign budget, we achieve up to 20 kW/h of emergency power to the surface habitat and maintain a global power supply of over 15 kW/h for rover exploration. Table 3 summarizes the key improvements to MARTEMIS mission objectives achieved through the addition of SBSP. This case study demonstrates SBSP as a valuable component of large mission architectures that prioritize long-term habitation, wide-range surface exploration, or otherwise high-risk human operations. In reducing risks associated with a single point-of-failure power system, SBSP provides operational flexibility, safety, and robustness to lunar exploration architectures.

Acknowledgements

Presenting authors Madelyn Hoying, Anna Tretiakova, and Vanessa Chen acknowledge travel support from the 2024 International Space Solar Power Student Competition, organized by SPACE Canada and the International Astronautical Federation (IAF) Power Committee. All authors acknowledge the MARTEMIS team and their advisors, in particular George Lordos, PhD, for the development and detailed analysis behind the MARTEMIS lunar architecture.

References

- [1] W. J. Larson and L. K. Pranke, *Human Spaceflight: Mission Analysis and Design*. McGraw-Hill New York, 2000.
- [2] National Aeronautics and Space Administration, *Moon to Mars Objectives*, 2022.
- [3] J. Applebaum and D. Flood, “Solar radiation on mars,” NASA Lewis Research Center, Tech. Rep., 1989.
- [4] National Aeronautics and Space Administration, *Fission surface power*, 2024.
- [5] Westinghouse Electric Company, *Evinci microreactor*, 2024.
- [6] U.S. Department of Defense, *DoD to Build Project Pele Mobile Microreactor and Perform Demonstration at Idaho National Laboratory*, 2022.
- [7] L. S. Mason, “A comparison of fission power system options for lunar and mars surface applications,” in *AIP Conference Proceedings*, American Institute of Physics, vol. 813, 2006, pp. 270–280.
- [8] J. M. Hickman and H. S. Bloomfield, “Comparison of solar photovoltaic and nuclear reactor power systems for a human-tended lunar observatory,” in *Proceedings of the 24th Intersociety Energy Conversion Engineering Conference*, IEEE, 1989, pp. 1–5.
- [9] F. Lopez, A. Mauro, S. Mauro, G. Monteleone, D. E. Sfasciamuro, and A. Villa, “A lunar-orbiting satellite constellation for wireless energy supply,” *Aerospace*, vol. 10, no. 11, p. 919, 2023.
- [10] A. Crocker, “Making human spaceflight practical and affordable: Spacecraft designs and their degree of operability,” in *AIAA SPACE 2011 Conference & Exposition*, 2011, p. 7336.
- [11] McKinney, Patel, Lordos, Hoying, *et al.*, “Martemis: Mars architecture research using taguchi experiments on the moon with international solidarity,” *NASA RASC-AL Technical Papers*, 2024.

- [12] G. Taguchi, "Performance analysis design," *The international journal of production research*, vol. 16, no. 6, pp. 521–530, 1978.
- [13] D. Akin, C. Hanner, N. Bolatto, D. Gribok, and Z. Lachance, "Design and development of an eva assistance roving vehicle for artemis and beyond," 50th International Conference on Environmental Systems, 2021.
- [14] D. A. Harrison, R. Ambrose, B. Bluethmann, and L. Junkin, "Next generation rover for lunar exploration," in *2008 IEEE aerospace conference*, IEEE, 2008, pp. 1–14.
- [15] A. F. Abercromby, M. L. Gernhardt, and H. Litaker, *Desert Research and Technology Studies (DRATS) 2009: A 14-day evaluation of the Space Exploration Vehicle prototype in a lunar analog environment*. National Aeronautics and Space Administration, Lyndon B. Johnson Space Center, 2012.
- [16] C. Fortezzo, P. Spudis, and S. Harrel, "Release of the digital unified global geologic map of the moon at 1: 5,000,000-scale," in *51st Annual Lunar and Planetary Science Conference*, 2020, p. 2760.
- [17] K. Kahoy, *L4 space geometry and orbits*, MIT AeroAstro 16.851 Satellite Engineering, 2020.
- [18] A. Konopliv, S. Asmar, E. Carranza, W. Sjogren, and D. Yuan, "Recent gravity models as a result of the lunar prospector mission," *Icarus*, vol. 150, no. 1, pp. 1–18, 2001.
- [19] M. Lara, B. De Saedeleer, and S. Ferrer, "Preliminary design of low lunar orbits," in *Proceedings of the 21st International Symposium on Space Flight Dynamics*, 2009, pp. 1–15.
- [20] Y. Zheng *et al.*, "Wireless laser power transmission: Recent progress and future challenges," *Space Solar Power and Wireless Transmission*, 2024.
- [21] ThorLabs, "Ytterbium-doped optical fiber," *ThorLabs Product Specifications*, 2024.
- [22] H. Ma, *Oscillating heat pipes*. Springer, 2015.
- [23] G. S. Nurre, S. J. Anhouse, and S. N. Gullapalli, "Hubble space telescope fine guidance sensor control system," in *Acquisition, Tracking, and Pointing III*, SPIE, vol. 1111, 1989, pp. 327–343.
- [24] H. Helmers *et al.*, "68.9% efficient gaas-based photonic power conversion enabled by photon recycling and optical resonance," *physica status solidi (RRL)–Rapid Research Letters*, vol. 15, no. 7, p. 2100113, 2021.
- [25] S. J. Boazman *et al.*, "The distribution and accessibility of geologic targets near the lunar south pole and candidate artemis landing sites," *The Planetary Science Journal*, vol. 3, no. 12, p. 275, 2022.
- [26] R. Wagner, M. Robinson, E. Speyerer, and J. Plescia, "Locations of anthropogenic sites on the moon," in *Lunar and planetary science conference*, 2014, p. 2259.
- [27] F. Musavi and W. Eberle, "Overview of wireless power transfer technologies for electric vehicle battery charging," *IET Power Electronics*, vol. 7, no. 1, pp. 60–66, 2014.
- [28] G. Lordos, "Engineering robust and autocatalytic architectures for human missions to mars," Ph.D. dissertation, Massachusetts Institute of Technology, 2024.
- [29] G. Lordos *et al.*, "PALE RED DOT: A large, robust architecture for human settlements on mars," in *ASCEND 2023*, 2023, p. 4776.
- [30] A. D. A. Gil, D. Renwick, C. Cappelletti, and P. Blunt, "Methodology for optimizing a constellation of a lunar global navigation system with a multi-objective optimization algorithm," *Acta Astronautica*, vol. 204, pp. 348–357, 2023.
- [31] K. Wang *et al.*, "Multi-orbit lunar gnss constellation design with distant retrograde orbit and halo orbit combination," *Scientific Reports*, vol. 13, no. 1, p. 10158, 2023.
- [32] S. Fu *et al.*, "Review of recent progress on single-frequency fiber lasers," *JOSA B*, vol. 34, no. 3, A49–A62, 2017.
- [33] H. Benaroya, "Lunar habitats: A brief overview of issues and concepts," *Reach*, vol. 7, pp. 14–33, 2017.

1. Satellite Locations

Figures 6, 7, 8, 9, 10, 11, 12, and 13 show satellite coverage over representative locations of interest in two-minute intervals.

Using MATLAB R2024a Lunar Orbital Propagation tool, the exact times of when each satellite enters and leaves the transmission cone of each chosen location. This data was organized in Google sheets and Tables 6 - 13 display the times when various satellites are overhead, both individually by plane and in combinations of multiple planes. Each table shows exactly what satellite (number and plane) passes over top of the location at a given time. For example, in Table 6, at time 6:50:45, the following satellites are overhead: satellite 1 of plane 1, satellite 10 of plane 1, and satellite 8 of plane 2. A more complex example is in Table 10; at time 6:15:14 the following satellites are overhead: satellite 8 of plane 2, satellite 9 of plane 9, satellite 7 of plane 3 and satellite 8 of plane 3. Since both satellites numbered 8 are overhead at this time, there is a number two in the “all planes satellite” column. Each plane has a designated color (plane 1 is blue, plane 2 is green, and plane 3 is red).

2. Power Delivery Calculations

Figures 14, 15, 16, 17, 20, 21, 18, and 19 show power delivery to a receiver at a location of interest.

Using the data in Appendix A and the expected power supply of 0.2 kW per 2 minutes, Tables 14 - 21 show the power delivered to each location over the span of two hours. This time span was chosen because a complete orbit of all planes takes about 2 hours.

Plane 1 Satellites											Plane 3 Satellites											All Plane Satellites										
1	2	3	4	5	6	7	8	9	10	1	2	3	4	5	6	7	8	9	10	1	2	3	4	5	6	7	8	9	10			
31-Oct-1924 6:10:04	0	1	1	0	0	0	0	0	0																							
31-Oct-1924 6:10:14	0	1	1	0	0	0	0	0	0																							
31-Oct-1924 6:11:04	0	1	1	0	0	0	0	0	0																							
31-Oct-1924 6:12:52	0	1	0	0	0	0	0	0	0																							
31-Oct-1924 6:15:14	0	1	0	0	0	0	0	0	0																							
31-Oct-1924 6:17:36	1	1	0	0	0	0	0	0	0																							
31-Oct-1924 6:19:58	1	1	0	0	0	0	0	0	0																							
31-Oct-1924 6:22:20	1	1	0	0	0	0	0	0	0																							
31-Oct-1924 6:24:41	1	0	0	0	0	0	0	0	0																							
31-Oct-1924 6:27:03	1	0	0	0	0	0	0	0	0																							
31-Oct-1924 6:29:25	1	0	0	0	0	0	0	0	1																							
31-Oct-1924 6:31:47	1	0	0	0	0	0	0	0	1																							
31-Oct-1924 6:34:09	1	0	0	0	0	0	0	0	1																							
31-Oct-1924 6:36:31	0	0	0	0	0	0	0	0	1																							
31-Oct-1924 6:38:52	0	0	0	0	0	0	0	0	1																							
31-Oct-1924 6:41:14	0	0	0	0	0	0	0	0	1	1																						
31-Oct-1924 6:43:36	0	0	0	0	0	0	0	0	1	1																						
31-Oct-1924 6:45:58	0	0	0	0	0	0	0	0	1	1																						
31-Oct-1924 6:48:20	0	0	0	0	0	0	0	0	1	0																						
31-Oct-1924 6:50:42	0	0	0	0	0	0	0	0	1	0																						
31-Oct-1924 6:53:03	0	0	0	0	0	0	0	1	1	0																						
31-Oct-1924 6:55:25	0	0	0	0	0	0	0	1	1	0																						
31-Oct-1924 6:57:47	0	0	0	0	0	0	0	1	1	0																						
31-Oct-1924 7:00:09	0	0	0	0	0	0	0	1	1	0																						
31-Oct-1924 7:02:31	0	0	0	0	0	0	0	1	0	0																						
31-Oct-1924 7:04:53	0	0	0	0	0	0	0	1	1	0																						
31-Oct-1924 7:07:15	0	0	0	0	0	0	0	1	1	0																						
31-Oct-1924 7:09:36	0	0	0	0	0	0	0	1	1	0																						
31-Oct-1924 7:11:58	0	0	0	0	0	0	0	1	0	0																						
31-Oct-1924 7:14:20	0	0	0	0	0	0	0	1	0	0																						
31-Oct-1924 7:16:42	0	0	0	0	0	0	0	1	1	0																						
31-Oct-1924 7:19:04	0	0	0	0	0	0	0	1	0	0																						
31-Oct-1924 7:21:26	0	0	0	0	0	0	0	1	0	0																						
31-Oct-1924 7:23:47	0	0	0	0	0	0	0	1	0	0																						
31-Oct-1924 7:26:09	0	0	0	0	0	0	0	1	0	0																						
31-Oct-1924 7:28:31	0	0	0	0	0	0	0	1	1	0																						
31-Oct-1924 7:30:53	0	0	0	0	0	0	0	1	1	0																						
31-Oct-1924 7:33:15	0	0	0	0	0	0	0	1	0	0																						
31-Oct-1924 7:35:37	0	0	0	0	0	0	0	1	0	0																						
31-Oct-1924 7:37:58	0	0	0	0	0	0	0	1	0	0																						
31-Oct-1924 7:40:20	0	0	0	0	0	0	0	1	0	0																						
31-Oct-1924 7:42:42	0	0	0	0	0	0	0	1	0	0																						
31-Oct-1924 7:45:04	0	0	0	0	0	0	0	1	0	0																						
31-Oct-1924 7:47:26	0	0	0	0	0	0	0	1	0	0																						
31-Oct-1924 7:49:48	0	0	0	0	0	0	0	1	0	0																						
31-Oct-1924 7:52:09	0	0	0	0	0	0	0	1	0	0																						
31-Oct-1924 7:54:31	0	0	0	0	0	0	0	1	0	0																						
31-Oct-1924 7:56:53	0	0	0	0	0	0	0	1	0	0																						
31-Oct-1924 7:59:15	0	0	0	0	0	0	0	1	0	0																						
31-Oct-1924 8:01:37	0	0	0	0	0	0	0	1	0	0																						
31-Oct-1924 8:03:59	0	0	0	0	0	0	0	1	0	0																						
31-Oct-1924 8:06:21	0	0	0	0	0	0	0	1	0	0																						
31-Oct-1924 8:08:16	0	0	0	0	0	0	0	1	0	0																						

Fig. 7. Apollo 12

A large data table with columns labeled 'Plane 2 Satellites', 'Plane 3 Satellites', and 'All Plane Satellites', each followed by sub-columns 1-10. The rows contain time-stamped data points from 31-Oct-1924 6:10:04 to 31-Oct-1924 8:08:16. The data values are binary (0 or 1) and are color-coded in green, red, or yellow.

Fig. 10. Artemis: Malapert Massif

Power (kW) Delivered Over Two Hours to Apollo 11 Location

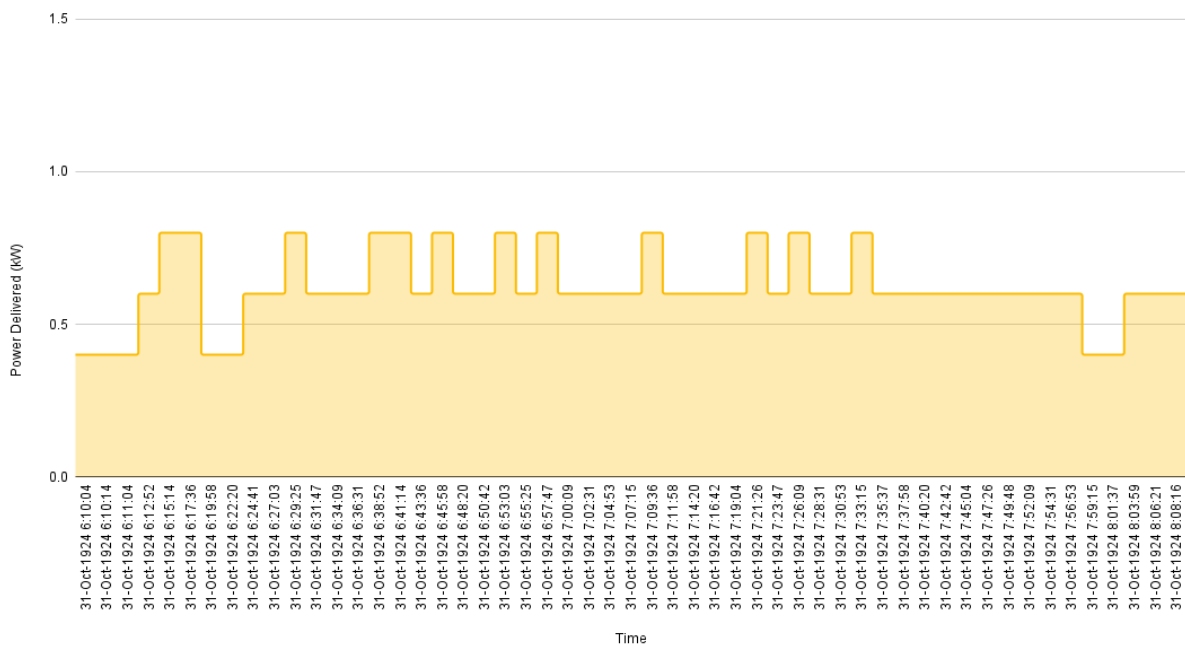


Fig. 14. Apollo 11

Power (kW) Delivered Over Two Hours to Apollo 12 Location

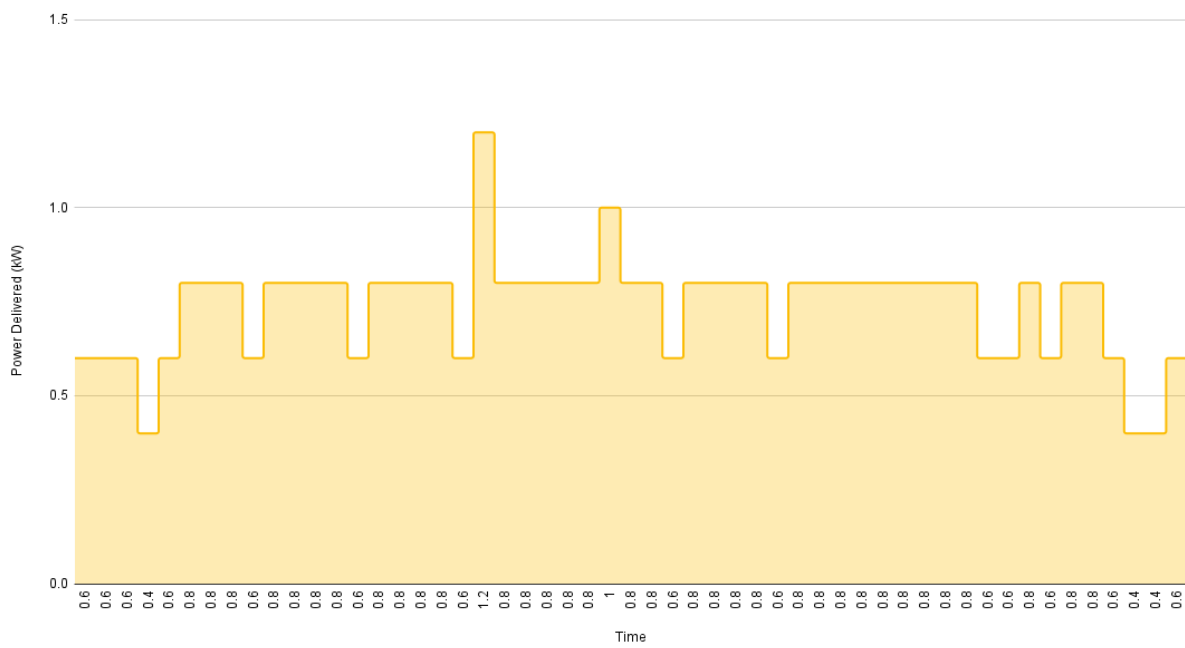


Fig. 15. Apollo 12

Power (kW) Delivered Over Two Hours to Apollo 16 Location

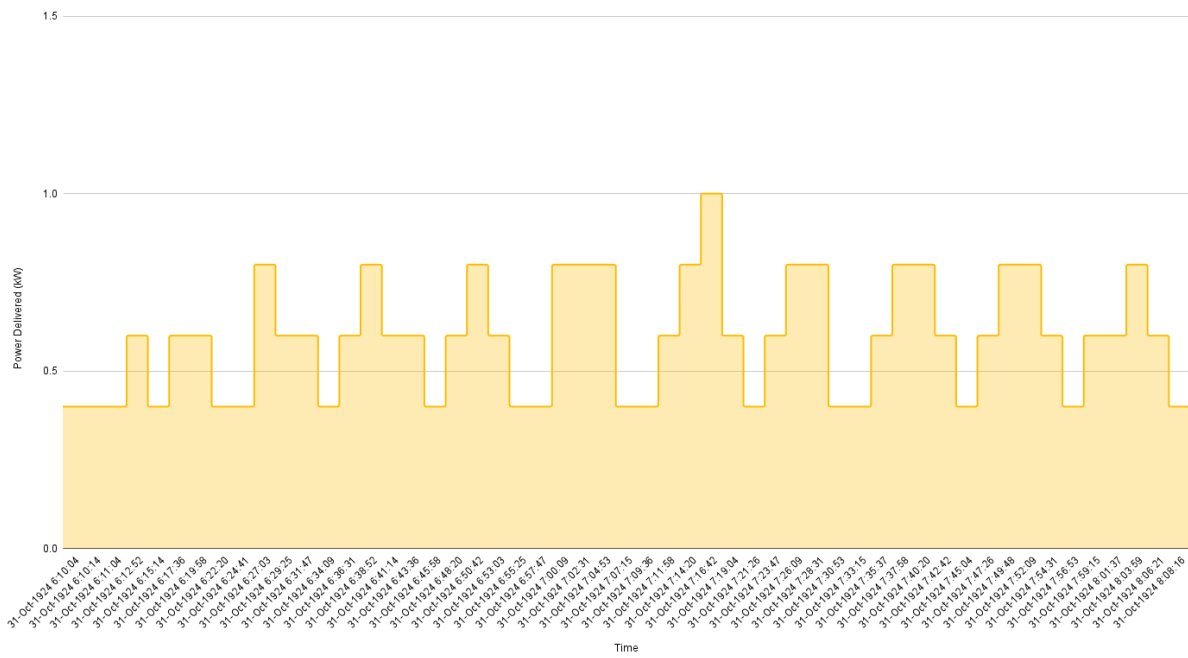


Fig. 16. Apollo 16

Power (kW) Delivered Over Two Hours to Apollo 17 Location

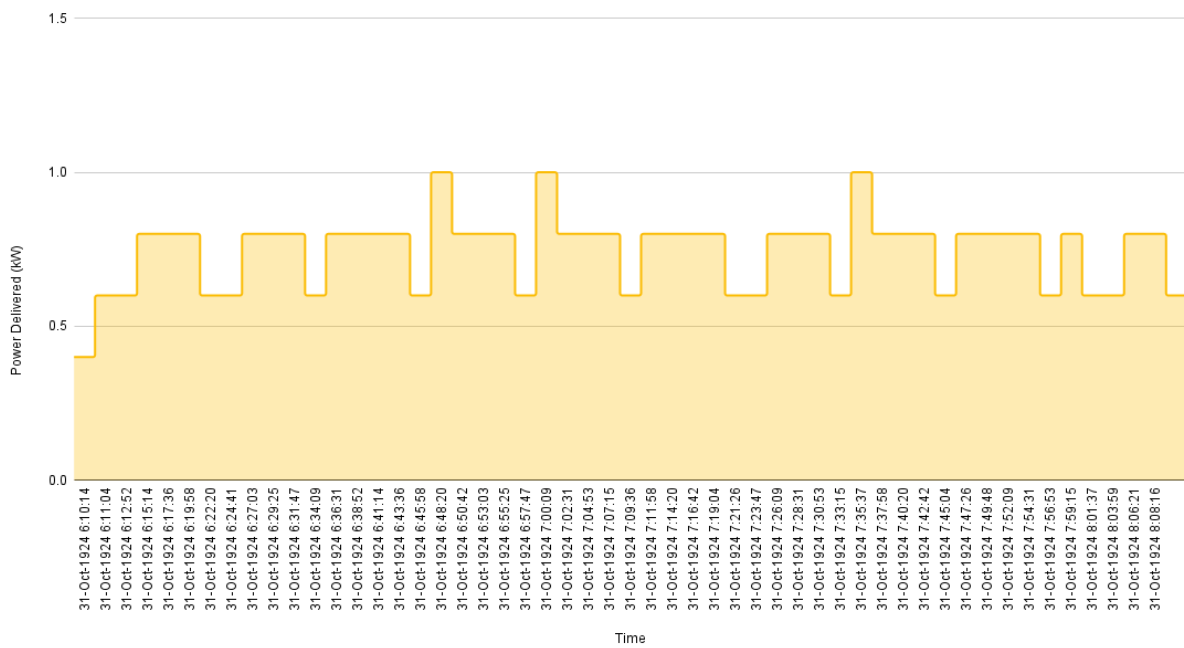


Fig. 17. Apollo 17

Power (kW) Delivered Over Two Hours to Malapert Massif Artemis Location

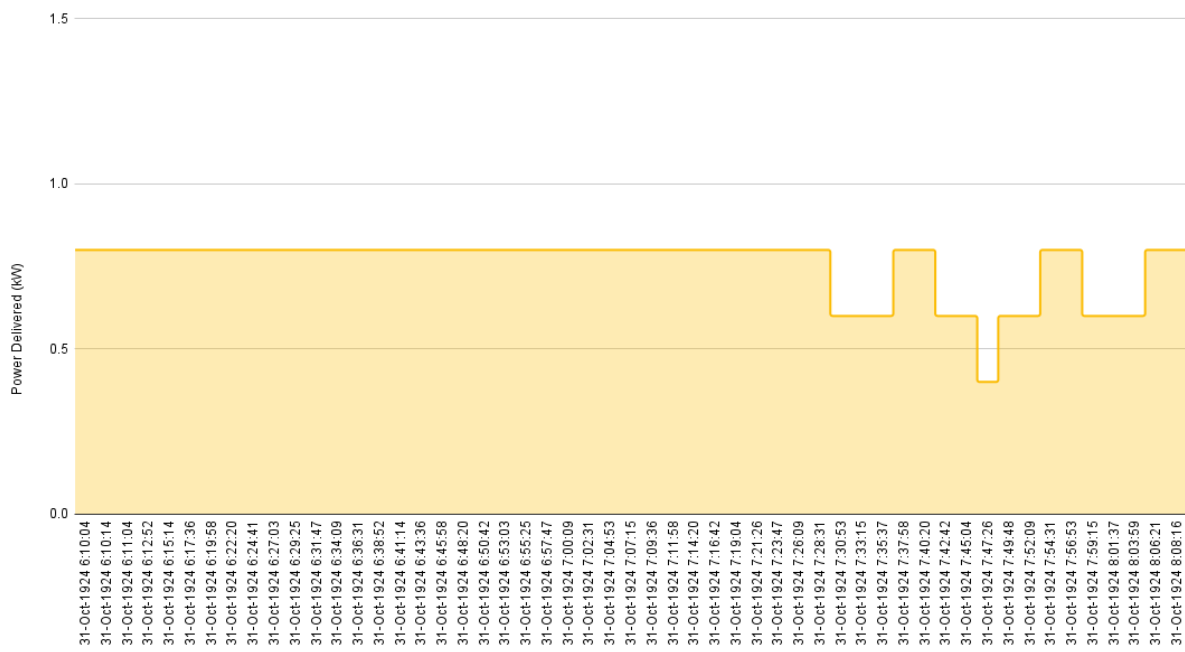


Fig. 18. Artemis: Malapert Massif

Power (kW) Delivered Over Two Hours to Peak Near Shackleton Artemis Location

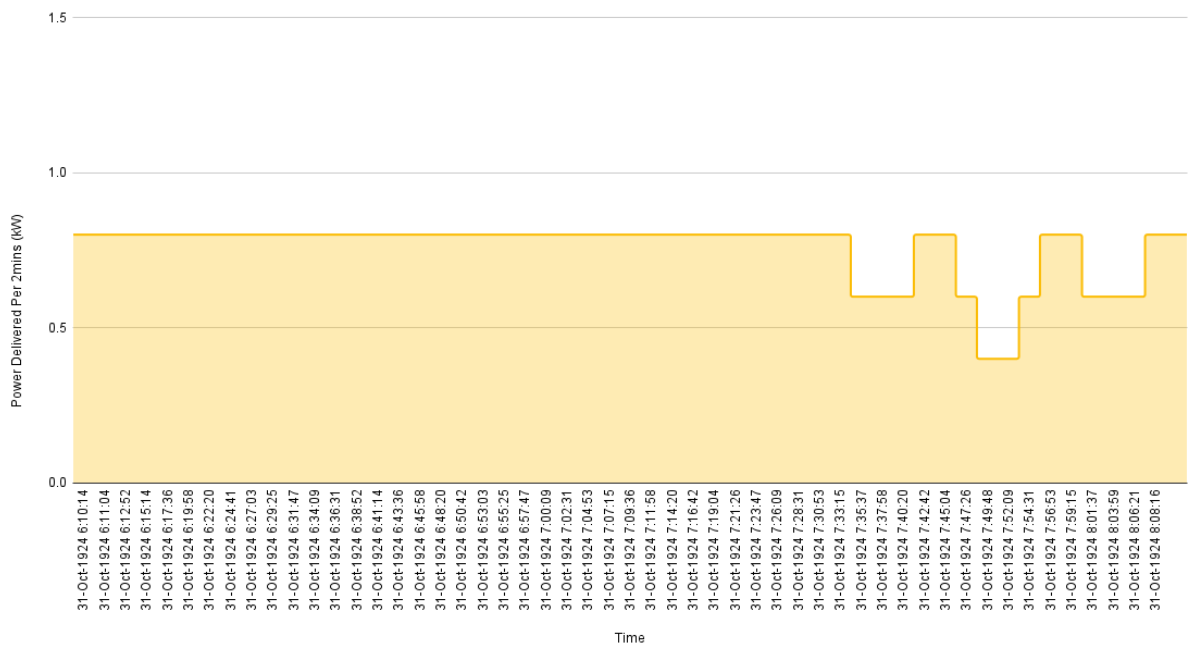


Fig. 19. Artemis: Shackleton

Power (kW) Delivered Over Two Hours to Amundsen Rim Artemis Location

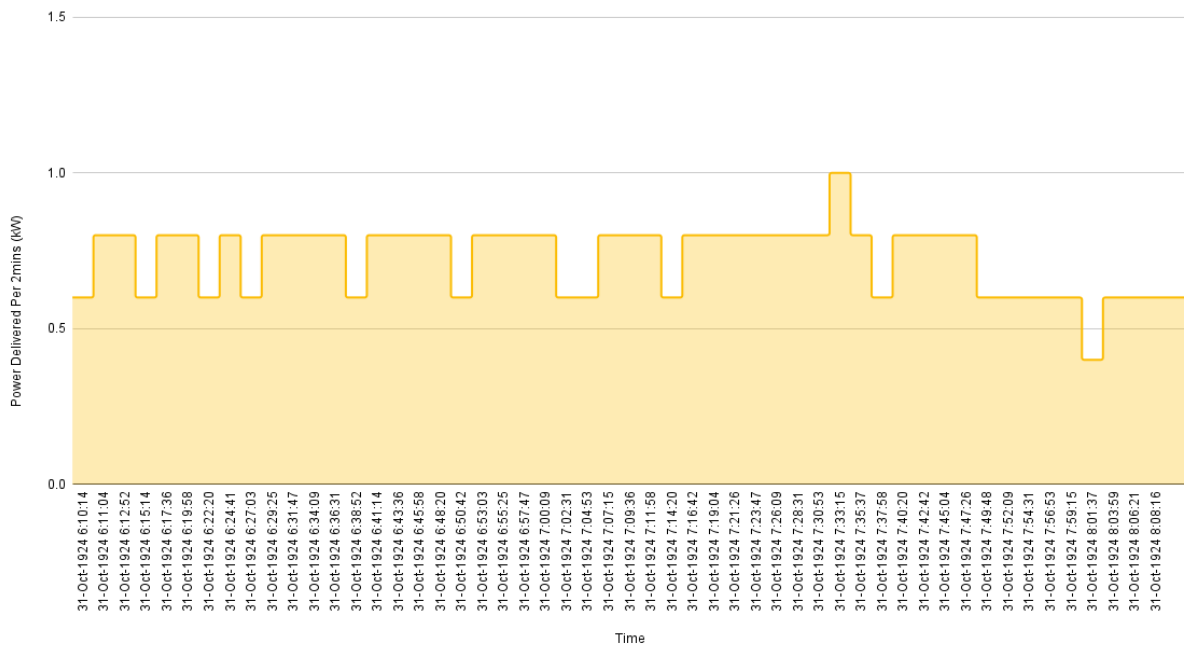


Fig. 20. Artemis: Amundsen Rim

Power (kW) Delivered Over Two Hours to de Gerlache-Kocher Massif Artemis Location

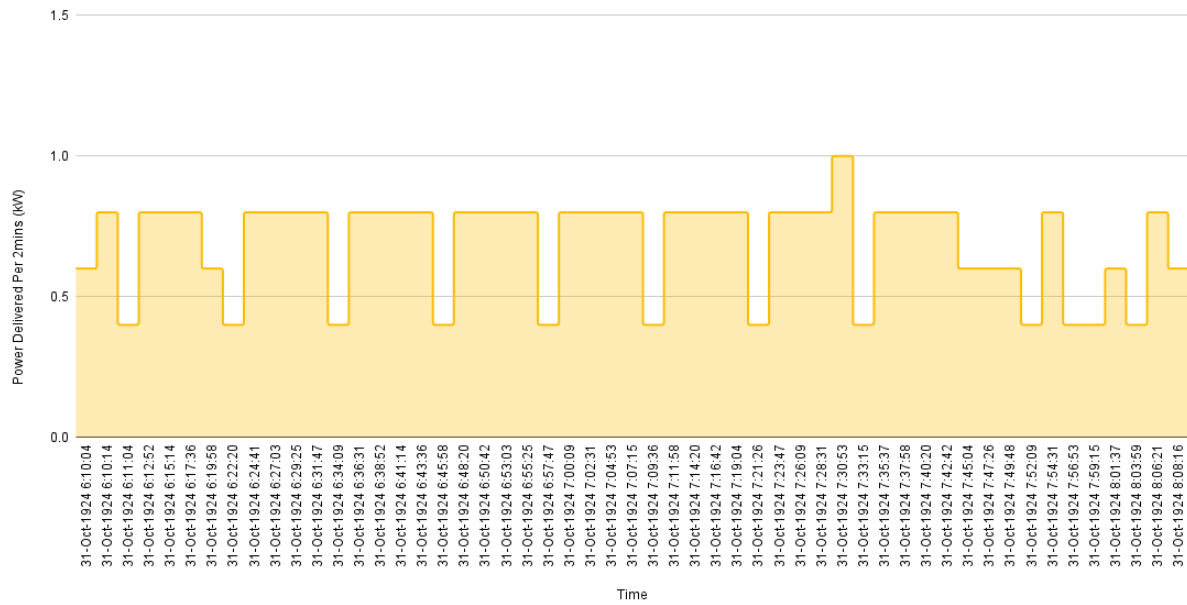


Fig. 21. Artemis: de Gerlache-Kocher Massif